View metadata, citation and similar papers at core.ac.uk

brought to you by CORE

provided by Elsevier - Publisher Connector

Physics Letters B 734 (2014) 255–260

Contents lists available at ScienceDirect

Physics Letters B

www.elsevier.com/locate/physletb

Critical endpoint and inverse magnetic catalysis for finite temperature and density quark matter in a magnetic background

M. Ruggieri [a,*], L. Oliva [a,b], P. Castorina [a,c], R. Gatto [d], V. Greco [a,b]

[a] Department of Physics and Astronomy, University of Catania, Via S. Sofia 64, I-95125 Catania, Italy
[b] INFN-Laboratori Nazionali del Sud, Via S. Sofia 62, I-95123 Catania, Italy
[c] INFN-CT, Via S. Sofia 62, I-95123 Catania, Italy
[d] Departement de Physique Theorique, Universite de Geneve, CH-1211 Geneve 4, Switzerland

ARTICLE INFO

Article history:
Received 10 February 2014
Received in revised form 15 May 2014
Accepted 25 May 2014
Available online 29 May 2014
Editor: J.-P. Blaizot

Keywords:
Chiral transition with finite magnetic background and chemical potential
Ginzburg–Landau effective action

ABSTRACT

In this article we study chiral symmetry breaking for quark matter in a magnetic background, $\boldsymbol{B}$, at finite temperature and quark chemical potential, μ, making use of the Ginzburg–Landau effective action formalism. As a microscopic model to compute the effective action we use the renormalized quark–meson model in the chiral limit. Our main goal is to study the evolution of the critical endpoint, $\mathcal{CP}$, as a function of the magnetic field strength, and investigate the realization of inverse magnetic catalysis at finite chemical potential. We find that the phase transition at zero chemical potential is always of the second order; for small and intermediate values of $\boldsymbol{B}$, $\mathcal{CP}$ moves towards small μ, while for larger $\boldsymbol{B}$ it moves towards moderately larger values of μ. Our results are in agreement with the inverse magnetic catalysis scenario at finite chemical potential and not too large values of the magnetic field, while at larger $\boldsymbol{B}$ direct magnetic catalysis sets in.

© 2014 The Authors. Published by Elsevier B.V. This is an open access article under the CC BY license (http://creativecommons.org/licenses/by/3.0/). Funded by SCOAP[3].

1. Introduction

Simulations of ultrarelativistic heavy ion collisions suggested the possibility that huge magnetic fields are created during non-central collisions [1–3]. The current estimate for the largest magnetic field produced is in the range $eB/m_\pi^2 \approx 5$–15, where m_π corresponds to the pion mass in the vacuum (to $eB = m_\pi^2$ corresponds $B \approx 10^{14}$ T). These results triggered the study of the modifications of a strong background field produces on spontaneous chiral symmetry breaking of Quantum Chromodynamics (QCD) and on deconfinement, both at zero and finite baryon density; for recent studies, as well as for some older results, see [4–26,28–31,27,34,33,32,35–37]. The existence of strong fields in heavy ion collisions, combined to the excitation of QCD sphalerons at high temperature, suggested the possibility of the Chiral Magnetic Effect [1,38], see [4] for reviews. Besides heavy ion collisions, even stronger magnetic fields might have been produced in the early universe at the epoch of the electroweak phase transition, t_{ew} [39,40]: a widely accepted value for the magnetic field at the transition is $B(t_{ew}) \approx 10^{19}$ T, even if this value has rapidly decreased scaling as a^{-2}, where $a(t)$ denotes the scale factor of the expanding universe, losing several order of magnitude at the QCD phase transition. Finally, relatively strong magnetic fields are relevant for magnetars, $B \approx 10^{10}$ T [41]. Therefore, there exist three physical contexts in which QCD in a strong magnetic background is worth to be studied.

In this Letter, we address the problem of the chiral phase transition for quark matter at finite quark chemical potential, μ, and nonzero magnetic field, $\boldsymbol{B}$, focusing on the critical endpoint, $\mathcal{CP}$, of the phase diagram where a second order and a first order transition lines meet each other, and on the chiral phase transition at finite μ. In order to make quantitative predictions we build up a Ginzburg–Landau (GL) effective potential for the chiral condensate as in [36] with the inclusion of a finite μ, beside T and $\boldsymbol{B}$ already considered in [36]. We work in the chiral limit since only in this case it is possible to define a phase transition, making the study within the GL expansion meaningful. Nevertheless the inclusion of a small explicit chiral symmetry breaking term should not modify the qualitative picture we obtain and explain in this Letter.

Even if we restrict ourselves to the case of a homogeneous condensate, the computation of the GL effective action has revealed a powerful tool to study the transitions to inhomogeneous phases when these are of the second order [42], beside more general treatments relying on heat kernel expansion techniques [43]. In [42] the coefficients of the GL potential are connected to those entering in the gradient expansion terms as well, which eventually

* Corresponding author.
E-mail address: marco.ruggieri@lns.infn.it (M. Ruggieri).

http://dx.doi.org/10.1016/j.physletb.2014.05.073
0370-2693/© 2014 The Authors. Published by Elsevier B.V. This is an open access article under the CC BY license (http://creativecommons.org/licenses/by/3.0/). Funded by SCOAP[3].

trigger inhomogeneous condensation. Hence our calculations pave the way for an efficient computation of second order transitions to inhomogeneous condensates at finite $\boldsymbol{B}$ and μ. For the mapping of the phase diagram from the space of the GL coefficients to the T–μ–$\boldsymbol{B}$ space we need a microscopic model to compute the explicit dependence of the GL coefficients on these variables. In this Letter we make use of the renormalized quark–meson model [46–49]. The advantage of this model is its renormalizability, which allows to make quantitative predictions which are not affected by any ultraviolet scale. It should be mentioned however that many effective chiral models fail to reproduce even qualitatively the behaviour of the critical temperature as a function of the magnetic field strength, besides few exceptions which are mentioned in Section 3 of this Letter, and this seems to be a robust claim as discussed in [57] where general modifications to the effective potential have been considered.

In [36] it was found that the critical point ($\mathcal{CP}$) at $\mu = 0$ is not in the phase diagram; hence it is of a certain interest to locate $\mathcal{CP}$ at finite μ and follow its evolution as the strength of $\boldsymbol{B}$ is increased. Moreover we wish to study the possible appearance of the phenomenon of inverse magnetic catalysis (IMC) at finite μ [25,19], that is the inhibition of spontaneous chiral symmetry breaking by the magnetic field. Our conclusions are that increasing the strength of $\boldsymbol{B}$ from zero to small values results in the evolution of $\mathcal{CP}$ towards smaller values of μ, but this tendency is reversed at strong $\boldsymbol{B}$. Hence within this model $\mathcal{CP}$ does not hit the $\mu = 0$ axis in the T–μ–$\boldsymbol{B}$ space. Moreover we confirm the predicted IMC scenario for small values of $\boldsymbol{B}$, at the same time offering a simple interpretation of this phenomenon. On the other hand, for larger values of eB we find direct magnetic catalysis at finite μ, that is, spontaneous chiral symmetry breaking is favoured by the magnetic field.

2. The model

In this work we use the renormalized quark–meson model as the microscopic model to compute the effective action at the chiral critical line. The model and its renormalization have been already presented in detail in a previous article [36], therefore here we remind only of the relevant definitions and steps of renormalization which will be used here.

The lagrangian density of the model is given by

$$\mathcal{L} = \bar{q}\big[iD_\mu\gamma^\mu - g(\sigma + i\gamma_5\boldsymbol{\tau}\cdot\boldsymbol{\pi})\big]q + \frac{1}{2}(\partial_\mu\sigma)^2 + \frac{1}{2}(\partial_\mu\boldsymbol{\pi})^2 - U(\sigma,\boldsymbol{\pi}). \tag{1}$$

In the above equation, q corresponds to a quark field in the fundamental representation of colour group $SU(N_c)$ and flavor group $SU(2)$; the covariant derivative, $D_\mu = \partial_\mu - Q_f eA_\mu$, describes the coupling to the background magnetic field, where Q_f denotes the charge of the flavor f. Besides, σ, $\boldsymbol{\pi}$ correspond to the scalar singlet and the pseudo-scalar iso-triplet fields, respectively. The potential U describes tree-level interactions among the meson fields,

$$U(\sigma,\boldsymbol{\pi}) = \frac{\lambda}{4}\big(\sigma^2 + \boldsymbol{\pi}^2 - v^2\big)^2, \tag{2}$$

which is invariant under chiral transformations.

We restrict ourselves to the one-loop approximation as in [36]. It has been shown in [20,35,19] that even including the quantum fluctuations by means of the functional renormalization group does not change the phase structure of the model. In the integration process, the meson fields are fixed to their classical expectation values, $\langle\boldsymbol{\pi}\rangle = 0$ and $\langle\sigma\rangle \neq 0$. The physical value of $\langle\sigma\rangle$ will be then determined by minimization of the thermodynamic potential. This implies the replacement $g\sigma \to g\langle\sigma\rangle$ in the quark action. The field σ carries the quantum numbers of the quark chiral condensate, $\langle\bar{q}q\rangle$; hence, in the phase with $\langle\sigma\rangle \neq 0$, chiral symmetry is spontaneously broken.

The one-loop thermodynamic potential associated to the interaction of fermions with a magnetic background can be computed within the Leung–Ritus–Wang method [50]:

$$\Omega_B = -N_c\sum_f \frac{|Q_f eB|}{2\pi}\sum_{n=0}^{\infty}\beta_n \times \int_{-\infty}^{+\infty}\frac{dp_z}{2\pi}\bigg[E + T\sum_{\gamma=\pm1}\log\big(1+e^{-\beta E_\gamma}\big)\bigg], \tag{3}$$

where n labels the Landau level, E corresponds to the single particle excitation spectrum,

$$E = \sqrt{p_z^2 + 2|Q_f eB|n + m_q^2}, \tag{4}$$

and $m_q = g\langle\sigma\rangle$ is the constituent quark mass. The factor $\beta_n = 2 - \delta_{n0}$ counts the degeneracy of the nth-Landau level. Finally $E_\gamma = \gamma\mu + E$.

The divergence in Ω_B is contained in the vacuum contribution. Since the model is renormalizable, we can treat this divergence by means of renormalization. In order to prepare Ω_B for renormalization we add and subtract the contribution at $\boldsymbol{B} = 0$, namely

$$\Omega_0 = -2N_cN_f\int\frac{d^3p}{(2\pi)^3}\bigg[\omega + T\sum_{\gamma=\pm1}\log\big(1+e^{-\beta\omega_\gamma}\big)\bigg], \tag{5}$$

where $\omega = \sqrt{\boldsymbol{p}^2 + m_q^2}$ and $\omega_\gamma = \mu\gamma + \omega$. This procedure is convenient since it allows to collect all the contributions due to the magnetic field into an addendum which is ultraviolet finite. Following the notation of [36] we split Ω_0 into the vacuum and the valence quark contributions, $\Omega_0 = \Omega_0^0 + \Omega_0^T$ with

$$\Omega_0^0 = -2N_cN_f\int\frac{d^3p}{(2\pi)^3}\omega, \tag{6}$$

$$\Omega_0^T = -2N_cN_fT\int\frac{d^3p}{(2\pi)^3}\sum_{\gamma=\pm1}\log\big(1+e^{-\beta\omega_\gamma}\big). \tag{7}$$

Hence we write

$$\Omega_B = \Omega_0 + (\Omega_B - \Omega_0) \equiv \Omega_0 + \delta\Omega. \tag{8}$$

In [10,36] it has been proved explicitly that $\delta\Omega$ is finite, modulo condensate independent terms, and it is not affected by renormalization. The condensate independent terms have been discussed in [16], where it is pointed out that they affect the renormalization procedure of electric charge and magnetic field, leaving however eB invariant; since eB is the only quantity which couples to fermions in our model, we can safely neglect this further renormalization. Removing the UV divergences requires the addition of two counterterms to the thermodynamic potential,

$$\Omega^{c.t.} = \frac{\delta\lambda}{4}\frac{m_q^4}{g^4} + \frac{\delta v}{2}\frac{m_q^2}{g^2}, \tag{9}$$

and the following renormalization conditions [8,10]

$$\frac{\partial(\Omega_0^0 + \Omega^{c.t.})}{\partial m_q}\bigg|_{m_q=gf_\pi} = \frac{\partial^2(\Omega_0^0 + \Omega^{c.t.})}{\partial m_q^2}\bigg|_{m_q=gf_\pi} = 0, \tag{10}$$

which amount to the requirement that the one-loop contribution in the vacuum, namely Ω_0^0, does not affect the expectation value of the scalar field and the mass of the scalar meson. The total thermodynamic potential thus reads

$$\Omega = \Omega_B + U + \Omega^{c.t.}. \tag{11}$$

3. Ginzburg–Landau expansion

In this section we present the novelty of our study. Our goal is to expand Ω in the Ginzburg–Landau (GL) form, in order to build up the effective potential at the critical line for the order parameter:

$$\Omega = \frac{\alpha_2}{2} m_q^2 + \frac{\alpha_4}{4!} m_q^4 + \frac{\alpha_6}{6!} m_q^6. \tag{12}$$

This will be useful to compute the chiral critical line at finite μ and $\boldsymbol{B}$. Given the thermodynamic potential in Eq. (11), the GL coefficients we need are obtained trivially as $\alpha_n = \partial^n \Omega / \partial m_q^n$ with derivative computed at $m_q = 0$. The $\boldsymbol{B}$-dependence of the GL coefficients comes only from $\delta\Omega$. In the case $\mu = 0$ we have found the analytical expressions for the GL coefficients [36]; on the other hand, for $\mu \neq 0$ this has not been possible because the presence of the quark chemical potential complicates the relevant momentum integrals. Therefore in this work we rely on a numerical evaluation of the GL coefficients. The kind of investigation we perform here is however still interesting: in fact in [36] it was found that at $\mu = 0$ the magnetic field does not induce a first order phase transition; on the other hand it is known that at $\boldsymbol{B} = 0$ and $\mu \neq 0$ a critical endpoint, $\mathcal{CP}$, appears for large enough values of μ, where the phase transition becomes of the first order. It is then of a certain interest to study how $\mathcal{CP}$ evolves at finite μ and $\boldsymbol{B}$ to understand its fate in the phase diagram as both $\boldsymbol{B}$ and μ are in the game. Moreover, the computation of α_4 will be crucial to explain the evolution of $\mathcal{CP}$ at finite μ, as we will discuss in the next section.

Before presenting the numerical results for the general case $\boldsymbol{B} \neq 0$ and $\mu \neq 0$ it is useful to remind of a few particular results. The critical temperature of a second order phase transition is obtained as a solution of the equation $\alpha_2 = 0$; at $\mu = 0$ and $\boldsymbol{B} = 0$ this condition implies [36]

$$T_c^2 = \frac{6\lambda v^2}{g^2 N_c N_f} + \frac{3 g^2 f_\pi^2}{2\pi^2}. \tag{13}$$

For a numerical estimate we take the parameters of [18], namely $\lambda = 20$, $v = f_\pi$ and $g = 3.3$; with this parameter set we find $T_c \approx 173$ MeV. In the above equation no UV cutoff appears, as it would appear instead in NJL or NJL-like models, see for example [51]. In our calculation the UV cutoff dependence has been removed by the renormalization and the only mass scale determining T_c is f_π. Numerical estimate of T_c in our case however is in agreement with the NJL calculations. In the case of a very strong magnetic field the critical temperature can be obtained by looking at α_2 in [36]; we obtain

$$T_c^2 = 2 Q_u^{Q_u} |Q_d|^{|Q_d|} |eB|, \tag{14}$$

which shows that $T_c \propto \sqrt{eB}$. This result is in contradiction with recent lattice computations [5], where it is found that in QCD T_c decreases with the increase of eB. This disagreement is most probably due to the lack of an appropriate description of the gluon sector in the present model. It is however possible to improve the model itself in order to describe the gluon backreaction to the magnetic field, thus reproducing at least qualitatively the behaviour of the critical temperature, see [45,32]. A critical temperature with the correct qualitative behaviour has been also obtained in [24] within the context of the large-N_c limit of QCD, as well as of the bag model (see also [13]), suggesting that the driving transition is the deconfinement one. We will not insist on these topics in this Letter, leaving them to future studies.

We close this section by mentioning that the use of the GL expansion we consider in this Letter is very important to understand, qualitatively and quantitatively, the response of the critical lines to the magnetic field, with particular reference to the critical endpoint evolution, as it will be clear from the results in the next section.

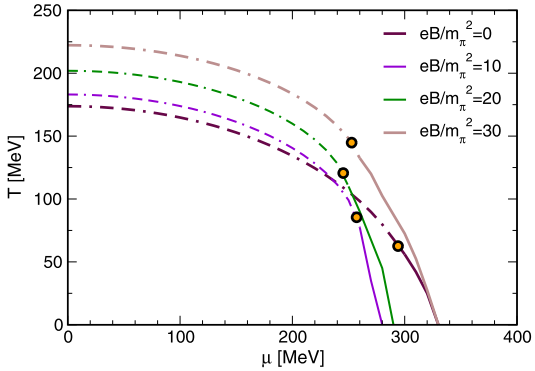

Fig. 1. Critical lines in the T–μ plane for several values of eB. Dashed lines correspond to second order transitions, solid lines to first order transitions. The critical endpoints for the different values of eB are denoted by dots. (For interpretation of the references to colour in this figure legend, the reader is referred to the web version of this article.)

4. Phase diagram and critical endpoint

In Fig. 1 we plot the phase diagram for spontaneous chiral symmetry breaking in the T–μ plane. Dashed lines correspond to second order critical lines, that are computed by solving the equation $\alpha_2(T_c, \mu, eB) = 0$. As in previous model studies in which the vacuum contribution to the free energy is taken into account, the critical temperature at zero and small μ is found to increase for increasing magnetic field strength. As already said, this is not in agreement with recent lattice data which instead predict that T_c becomes smaller for increasing value of eB; it is clear that this discrepancy is not due to the lack of quantum fluctuations in the present model calculations, see [20,35,19]. Among the several possibilities suggested for the interpretation of this problem [44,45,32] the one closer to our work which does not require the introduction of a Polyakov loop background is given in [45] where an axial chemical potential, μ_5, is added and its magnitude is assumed to be an increasing function of eB, this dependence being inspired by previous works which show that a large value of eB increases the fluctuations of chiral charge [23] and the sphaleron rate [52]. In fact a finite μ_5 is found to decrease the temperature of chiral symmetry restoration [17,53,54]. In the model at hand it is possible to add the axial chemical potential, following the line of previous works within NJL as well as quark–meson model [17,53,54]. We will not consider this further complication here, leaving the inclusion of μ_5 to a future project.

For completeness in Fig. 1 we have also drawn the first order phase transition lines. First order lines might be computed by the potential in Eq. (12); however the GL expansion is not expected to be quantitatively reliable at a first order line because the condensate might be still large at the phase transition; therefore in order to compute those lines we have used the full renormalized thermodynamic potential. Finally, the dots in the figure denote the critical endpoints.

The critical lines depicted in Fig. 1 are in agreement with the scenario of inverse magnetic catalysis (IMC) at finite μ [25,19]. More precisely for small and moderate values of eB and large enough μ the critical temperature decreases with increasing eB. For large values of eB instead this IMC tendency seems to disappear and magnetic catalysis takes place. Restricting the discussion to $T = 0$ the IMC is evident for small fields since the critical value for chiral symmetry restoration, μ_c, decreases for increasing eB.

For larger values of the magnetic field instead we find that μ_c increases against eB. We can give handwaving arguments about why this phenomenon takes place within the model. In this discussion it is useful to remind that μ_c is expected to be of the order of m_q.

In the model at hand, the restoration of chiral symmetry is due to the accommodation of valence quarks into single particle states, a process causing an increase of free energy that can be read from Eq. (3), namely

$$\Delta\Omega_{vq} = \frac{N_c|eB|}{2\pi^2}\sum_f |Q_f| \sum_{n=0}^{\infty}\beta_n \int_0^{+\infty} dp_z \theta(\mu - E)(E-\mu). \tag{15}$$

The above contribution is finite and not affected by renormalization. The θ-function in Eq. (15) makes the integral nonvanishing only when the condition $\mu^2 > m_q^2$ is satisfied. Moreover it implies that both the conditions $\mu^2 - m_q^2 > 2|eB|n$ and $\mu^2 - m_q^2 - 2|eB|n > p_z^2$ have to be satisfied. To measure energies from a common point we subtract from Eq. (15) the analogous contribution at $m_q = 0$, since it corresponds to an irrelevant constant which does not modify the value of the condensate and the transition point. Therefore we define

$$\delta\Omega_{vq} = \Delta\Omega_{vq} - \Delta\Omega_{vq}(m_q = 0). \tag{16}$$

Restricting to values of $\mu \approx m_q$ corresponding to the regime where we expect a phase transition, the free energy gain corresponding to the accommodation of quarks into the phase space is

$$\delta\Omega_{vq} = \frac{N_c}{4\pi^2}|eB|m_q^2, \tag{17}$$

which can be derived from Eq. (15) noticing that the restrictions imposed by the θ-function imply, for $\mu \approx m_q$, that only the lowest Landau level (LLL) gives a contribution to the sum if eB is not too small. Eq. (17) shows that the free energy gain for accommodating valence quarks in the phase space is $\sim |eB|m_q^2$. On the other hand, if eB is small enough then the renormalized condensation free energy loss due to condensation in the magnetic field is [10]

$$\delta\Omega_c = -\frac{N_c}{24\pi^2}(eB)^2 \log\frac{m_q}{\lambda}, \tag{18}$$

where λ plays the role of an infrared scale which does not affect the condensate. We mention that despite the appearance the $m_q \to 0$ limit in the above equation is not singular, since the equation is valid in the asymptotic regime $m_q^2/eB \gg 1$ hence the small mass limit cannot be taken. The effective potential is not singular in the $m_q \to 0$ limit as it can be proved following the calculations in [10]. The above equation corresponds to a negative contribution to the free energy meaning that it favours the breaking of chiral symmetry because it lowers the value of Ω. It is easy to check that in this weak field limit, because of $m_q = gf_\pi + \delta m_q(eB)$ with $\delta m_q(eB) \sim (eB)^2/f_\pi^3$ [10], the further contributions to the condensation energy in the magnetic background arising from U and Ω_0^0 are of the order $(eB)^4$ hence negligible compared to Eq. (18). Comparing Eqs. (17) and (18) we realize that the stabilization in creating a condensate in the magnetic background is parametrically smaller than the destabilization induced by the accommodation of valence quarks, therefore the net effect of the magnetic field will be to increase the free energy of the condensed phase favouring the restoration of chiral symmetry.

On the other hand in the limit $eB \gg \mu^2$ the free energy loss due to condensation in the magnetic field is given by [10]

$$\delta\Omega_c = -\frac{N_c}{8\pi^2}m_q^2|eB|\log\frac{|eB|}{m_q^2}; \tag{19}$$

the free energy gain $\delta\Omega_{vq}$ is still given by Eq. (17). In the strong field limit we realize a competition takes place between free energy loss Eq. (19) and gain Eq. (18), both being of order $|eB|m_q^2$; moreover $\delta\Omega_c$ gets a logarithm enhancement for very large values of eB, which results eventually in lowering the free energy of the condensate phase enhancing chiral symmetry breaking. In this limit we expect catalysis of chiral symmetry breaking with μ_c^2 proportional to $|eB|$, which explains why we find that μ_c increases with eB for large enough values of eB. It is useful to notice that in the case we do not renormalize the model and keep a finite value of the cutoff, Λ, then the logarithm in Eq. (19) is replaced by a function of m_q/Λ as it can be proved easily from Eq. (3) in LLL approximation; in this case $\delta\Omega_c$ is still of the order of $|eB|m_q^2$ but it is not easy to predict the fate of μ_c because the dependence of m_q on eB makes the comparison of $\delta\Omega_c$ and $\delta\Omega_{vq}$ less transparent.

In Fig. 1 the dots denote the critical endpoint, $\mathcal{CP}$, in the T–μ plane for several values of eB. $\mathcal{CP}$ is defined as the intersection of a second order and a first order transition lines: for each value of eB the $\mathcal{CP}$ coordinates are located by solving the equations $\alpha_2(T,\mu,eB) = \alpha_4(T,\mu,eB) = 0$. The evolution of $\mathcal{CP}$ depicted in Fig. 1 is quite peculiar since it shows that increasing the value of eB then $\mathcal{CP}$ does not hit the axis $\mu = 0$; rather it evolves towards large temperature and chemical potential. The absence of $\mathcal{CP}$ at $\mu = 0$ even for large magnetic fields can be understood at the light of the results of [36]: at $\mu = 0$ and very large eB it has been found

$$\alpha_4 \propto |eB|/T^2, \tag{20}$$

showing that the quartic coefficient of the GL expansion is always positive, hence making the transition at $\mu = 0$ a second order one for any value of eB. The result in Eq. (20) is obtained within the renormalized model; the use of an explicit cutoff makes α_4 negative at large enough T, thus turning the transition to a first order and a critical point appears also at $\mu = 0$. If we use a fixed cutoff we expect thus that $\mathcal{CP}$ evolves towards the $\mu = 0$ axis for large enough eB. However we do not insist on this aspect because we are interested in the phase structure of the renormalized model in which no explicit ultraviolet cutoff is present. As a final comment we notice that the evolution of $\mathcal{CP}$ in Fig. 1 is in agreement with an independent calculation making use of a model which takes into account the Polyakov loop thermodynamics [33].

The evolution of $\mathcal{CP}$ in the T–μ plane as a function of eB in the model can be easily understood. For concreteness we refer to $eB/m_\pi^2 = 10$ and to $eB/m_\pi^2 = 30$, because in between these two values of eB the turning of $\mathcal{CP}$ evolution takes place. For the discussion the magnetic field dependent contribution to α_4, which we call $\delta\alpha_4$, have to be considered, and $\alpha_4 = \alpha_4^0 + \delta\alpha_4$ with $\alpha_4^0 = \alpha_4(\boldsymbol{B} = 0)$. We have checked that for the aforementioned values of magnetic field the higher Landau levels do not give a significant contribution to $\delta\alpha_4$ in the critical region, therefore we do not include them in the following discussion. In this case only the LLL contribution to $\delta\alpha_4$ is necessary; a computation similar to that presented in [36] leads to the result

$$\delta\alpha_4 = \frac{3N_c a_4}{\pi^2}\frac{|eB|}{T^2} f(\mu/T), \tag{21}$$

and $a_4 \approx 0.11$. The function f is shown in Fig. 2; in the $\mu \to 0$ limit Eq. (21) gives the result of [36]. For $eB/m_\pi^2 = 10$ the values of μ/T around $\mathcal{CP}$ are large enough to make f negative, while α_4^0 is positive. This means that LLL lowers the value of α_4 favouring a first order phase transition. This explains why $\mathcal{CP}$ moves towards smaller values of μ. On the other hand for $eB/m_\pi^2 = 30$ we find that α_4^0 is suppressed compared to $\delta\alpha_4$ hence $\alpha_4 \approx \delta\alpha_4$; moreover the values of μ/T in the critical region are smaller because T_c is enhanced by the magnetic field, eventually bringing f to be

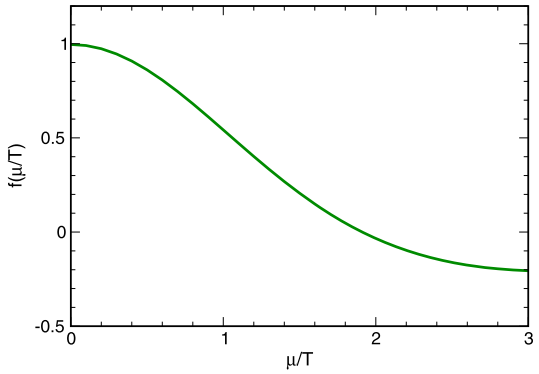

Fig. 2. Function f entering in Eq. (21).

positive. As a result, in this case the LLL favours a second order phase transition, thus pushing $\mathcal{CP}$ towards larger values of μ.

The evolution in Fig. 1 is quite interesting because it shows that increasing the strength of the magnetic field $\mathcal{CP}$ moves towards smaller values of μ for moderate values of eB, then changing this tendency for larger values of eB; this turning might suggest that the phase transition at $\mu = 0$ becomes stiffer for moderate values of eB then becomes softer, the stiffening and softening following the evolution of $\mathcal{CP}$. However this is not the case and the phase transition at $\boldsymbol{B} = 0$ becomes stiffer as eB becomes larger. In fact one way to measure stiffness of the phase transition is to compute $S \equiv |dm_q^2/dT|$ at $T = T_c$: from the potential (12) we get $m_q^2 = -6\alpha_2/\alpha_4$ (neglecting the α_6 term, which can be done at a second order phase transition), which for $T \lesssim T_c$ implies

$$S = -\frac{6}{\alpha_4(T_c)}\frac{d\alpha_2}{dT}\bigg|_{T=T_c}(T - T_c); \tag{22}$$

using the large field limit results of [10], namely $\alpha_2 \propto |eB| \times \log(|eB|/T^2)$ and $\alpha_4 \propto |eB|/T^2$, we get

$$S \propto \frac{|eB|}{T_c}, \tag{23}$$

which shows that the stiffness increases as $\sqrt{|eB|}$ since in the strong field limit $T_c \propto \sqrt{|eB|}$. In the weak field limit one has to take into account also the $\boldsymbol{B}$-independent contributions for α_2, α_4 but the correction to the stiffness due to the magnetic field is still given by Eq. (23) in which, at the lowest order, $T_c = T_c(\boldsymbol{B} = 0)$, showing that in the weak field limit S is enhanced as $|eB|$. Summarizing, we find that S increases with eB both in the weak and in the strong field limit; however the dependence on eB is stronger in the weak field limit and weaker in the case of strong fields.

5. Conclusions

In this article we have studied the phase structure of hot quark matter in a magnetic background, $\boldsymbol{B}$, at finite temperature, T, and quark chemical potential, μ, making use of the Ginzburg–Landau (GL) effective action formalism to compute the regions in the T–μ–eB space where chiral symmetry is spontaneously broken. As a microscopic model to compute the GL coefficients we have used the renormalized quark–meson model. The absence of an explicit ultraviolet cutoff permits a consistent calculation even for large μ as well as for large $|eB|$. Apart from the work [36] which anticipates the formalism and some of the results we obtain here, the renormalized quark–meson model has been used for calculating the mean field phase diagram at finite magnetic field and chemical potential in [31] where a similar phase pattern is found. However in [31] an attempt to understand the dynamics which leads to the evolution of the critical endpoint, as well as of the inverse magnetic catalysis at small temperature, is missing, and similar explanations are missing in all the previous studies. Hence our Letter aims to fill this gap: while reproducing previous results, we also give clear interpretations of them. We also mention that for what concerns the inverse magnetic catalysis, our argument is not dependent on particular values of the parameters of the model, hence our explanation should be quite general.

The results obtained here for the critical temperature are in agreement with previous studies based on different approaches. In particular we confirm the scenario of inverse magnetic catalysis (IMC) at finite μ up to moderate values of eB, in our calculations up to $eB \approx 10 m_\pi^2$; instead at large eB magnetic catalysis appears. The IMC at small eB is understood within this model because the decrease of free energy due to condensation in magnetic field is parametrically smaller than the increase of free energy necessary to accommodate valence quarks in the phase space: in fact at small eB for the former we have $\delta\Omega_c \sim -(eB)^2$ while for the latter $\delta\Omega_{vq} \sim m_q^2|eB|$ with $m_q \approx \mu$ at the phase transition. On the other hand at large eB the renormalized decrease of free energy due to condensation is $\delta\Omega_c \sim -m_q^2|eB|\log(|eB|/m_q^2)$ and competes with $\delta\Omega_{vq}$, eventually triggering magnetic catalysis thanks to the logarithm enhancement.

We have also computed the evolution of the critical endpoint $\mathcal{CP}$ in the T–μ–eB space. We have found that for small and intermediate values of eB, $\mathcal{CP}$ moves towards smaller values of μ; on the other hand for large values of eB the critical endpoint moves towards larger values of μ. We have explained this evolution in terms of the lowest Landau level contribution to the coefficient α_4 of the GL effective potential at finite μ and T, whose sign determines the order of the phase transition. This result agrees with the computation at $\mu = 0$ of [36] where it was found that the α_4 is always positive in the renormalized model at $\mu = 0$, thus favouring the scenario that at $\mu = 0$ the phase transition is of the second order also at large eB.

There are several directions which are worth to be considered for continuing the present work. Including an axial chemical potential following [53,54] is interesting in view of the possible role this quantity has to induce inverse magnetic catalysis at $\mu = 0$ [45], and study the interplay between μ and μ_5 which was investigated for the first time in [53]. Moreover, the extension of the GL effective action formalism to study inhomogeneous phases [42,55] (see [56] for a review) is with no doubt fascinating. Even more, the inclusion of the Polyakov loop thermodynamical contribution to the effective potential is of a certain interest because it might affect the GL effective action in a nontrivial way. We plan to study these topics in our future projects.

Acknowledgements

We acknowledge H. Abuki, M. D'Elia and M. Tachibana for their careful reading of the manuscript and useful comments on the first version of this Letter. V.G. acknowledges the ERC-STG funding under the QGPDyn grant.

References

[1] D.E. Kharzeev, L.D. McLerran, H.J. Warringa, Nucl. Phys. A 803 (2008) 227.
[2] V. Skokov, A.Y. Illarionov, V. Toneev, Int. J. Mod. Phys. A 24 (2009) 5925.
[3] V. Voronyuk, V.D. Toneev, W. Cassing, E.L. Bratkovskaya, V.P. Konchakovski, S.A. Voloshin, Phys. Rev. C 83 (2011), 054911.
[4] D. Kharzeev, K. Landsteiner, A. Schmitt, H.-U. Yee (Eds.), Strongly Interacting Matter in Magnetic Fields, Lecture Notes in Phys., Springer, 2013.
[5] G.S. Bali, et al., J. High Energy Phys. 1202 (2012), 044.
[6] S.P. Klevansky, R.H. Lemmer, Phys. Rev. D 39 (1989) 3478;
I.A. Shushpanov, A.V. Smilga, Phys. Lett. B 402 (1997) 351;
D.N. Kabat, K.M. Lee, E.J. Weinberg, Phys. Rev. D 66 (2002), 014004;
T. Inagaki, D. Kimura, T. Murata, Prog. Theor. Phys. 111 (2004) 371;
T.D. Cohen, D.A. McGady, E.S. Werbos, Phys. Rev. C 76 (2007), 055201.

[7] M. D'Elia, F. Negro, Phys. Rev. D 83 (2011), 114028;
G.S. Bali, et al., Phys. Rev. D 86 (2012), 071502.
[8] H. Suganuma, T. Tatsumi, Ann. Phys. 208 (1991) 470.
[9] V.P. Gusynin, V.A. Miransky, I.A. Shovkovy, Nucl. Phys. B 462 (1996) 249;
V.P. Gusynin, V.A. Miransky, I.A. Shovkovy, Nucl. Phys. B 563 (1999) 361;
G.W. Semenoff, I.A. Shovkovy, L.C.R. Wijewardhana, Phys. Rev. D 60 (1999), 105024;
V.A. Miransky, I.A. Shovkovy, Phys. Rev. D 66 (2002), 045006.
[10] M. Frasca, M. Ruggieri, Phys. Rev. D 83 (2011), 094024.
[11] K.G. Klimenko, Theor. Math. Phys. 89 (1992) 1161;
K.G. Klimenko, Teor. Mat. Fiz. 89 (1991) 211;
K.G. Klimenko, Z. Phys. C 54 (1992) 323;
K.G. Klimenko, Theor. Math. Phys. 90 (1992) 1;
K.G. Klimenko, Teor. Mat. Fiz. 90 (1992) 3.
[12] E.S. Fraga, A.J. Mizher, Phys. Rev. D 78 (2008), 025016.
[13] N.O. Agasian, S.M. Fedorov, Phys. Lett. B 663 (2008) 445.
[14] F. Bruckmann, G. Endrodi, T.G. Kovacs, J. High Energy Phys. 1304 (2013), 112.
[15] M. D'Elia, S. Mukherjee, F. Sanfilippo, Phys. Rev. D 82 (2010), 051501.
[16] G. Endrodi, arXiv:1301.1307 [hep-ph].
[17] K. Fukushima, M. Ruggieri, R. Gatto, Phys. Rev. D 81 (2010), 114031;
R. Gatto, M. Ruggieri, Phys. Rev. D 83 (2011), 034016;
R. Gatto, M. Ruggieri, Phys. Rev. D 82 (2010), 054027.
[18] A.J. Mizher, M.N. Chernodub, E.S. Fraga, Phys. Rev. D 82 (2010), 105016.
[19] J.O. Andersen, A. Tranberg, J. High Energy Phys. 1208 (2012), 002.
[20] V. Skokov, Phys. Rev. D 85 (2012), 034026.
[21] K. Fukushima, J.M. Pawlowski, Phys. Rev. D 86 (2012), 076013.
[22] M.N. Chernodub, Phys. Rev. D 82 (2010), 085011;
M.N. Chernodub, Phys. Rev. Lett. 106 (2011), 142003;
M.N. Chernodub, Phys. Rev. D 86 (2012), 107703;
V.V. Braguta, et al., Phys. Lett. B 718 (2012) 667.
[23] P.V. Buividovich, et al., Phys. Lett. B 682 (2010) 484;
P.V. Buividovich, et al., Nucl. Phys. B 826 (2010) 313;
P.V. Buividovich, et al., Phys. Rev. D 80 (2009), 054503.
[24] E.S. Fraga, L.F. Palhares, Phys. Rev. D 86 (2012), 016008;
E.S. Fraga, J. Noronha, L.F. Palhares, arXiv:1207.7094 [hep-ph];
J.-P. Blaizot, E.S. Fraga, L.F. Palhares, arXiv:1211.6412 [hep-ph].
[25] F. Preis, A. Rebhan, A. Schmitt, J. High Energy Phys. 1103 (2011), 033;
F. Preis, A. Rebhan, A. Schmitt, J. Phys. G 39 (2012) 054006.
[26] N. Callebaut, D. Dudal, arXiv:1303.5674 [hep-th];
N. Callebaut, D. Dudal, H. Verschelde, J. High Energy Phys. 1303 (2013), 033.
[27] A. Gynther, K. Landsteiner, F. Pena-Benitez, A. Rebhan, J. High Energy Phys. 1102 (2011), 110.
[28] J.O. Andersen, R. Khan, Phys. Rev. D 85 (2012), 065026;
J.O. Andersen, Phys. Rev. D 86 (2012), 025020;
J.O. Andersen, J. High Energy Phys. 1210 (2012), 005.
[29] P. Burikham, J. High Energy Phys. 1105 (2011), 121.
[30] V.G. Filev, R.C. Raskov, Adv. High Energy Phys. 2010 (2010) 473206;
G. Lifschytz, M. Lippert, Phys. Rev. D 80 (2009), 066007.
[31] G.N. Ferrari, A.F. Garcia, M.B. Pinto, Phys. Rev. D 86 (2012), 096005.
[32] M. Ferreira, P. Costa, D.P. Menezes, C. Providencia, N. Scoccola, Phys. Rev. D 89 (2014), 016002, arXiv:1305.4751 [hep-ph].
[33] P. Costa, M. Ferreira, H. Hansen, D.P. Menezes, C. Providencia, Phys. Rev. D 89 (2014), 056013, arXiv:1307.7894 [hep-ph].
[34] M. Ferreira, P. Costa, C. Providencia, Phys. Rev. D 89 (2014), 036006, arXiv:1312.6733 [hep-ph].
[35] K. Kamikado, T. Kanazawa, arXiv:1312.3124 [hep-ph].
[36] M. Ruggieri, M. Tachibana, V. Greco, J. High Energy Phys. 2013 (2013), 165.
[37] G. Colucci, E.S. Fraga, A. Sedrakian, Phys. Lett. B 728 (2014) 19.
[38] K. Fukushima, D.E. Kharzeev, H.J. Warringa, Phys. Rev. D 78 (2008), 074033;
K. Fukushima, D.E. Kharzeev, H.J. Warringa, Nucl. Phys. A 836 (2010) 311;
K. Fukushima, D.E. Kharzeev, H.J. Warringa, Phys. Rev. Lett. 104 (2010), 212001.
[39] T. Vachaspati, Phys. Lett. B 265 (1991) 258.
[40] L. Campanelli, Phys. Rev. Lett. 111 (2013), 061301.
[41] R.C. Duncan, C. Thompson, Astrophys. J. 392 (1992) L9.
[42] H. Abuki, D. Ishibashi, K. Suzuki, Phys. Rev. D 85 (2012), 074002;
H. Abuki, Phys. Rev. D 87 (2013), 094006;
H. Abuki, arXiv:1307.8173 [hep-ph].
[43] A. Flachi, T. Tanaka, J. High Energy Phys. 1102 (2011), 026;
A. Flachi, J. High Energy Phys. 1201 (2012), 023.
[44] T. Kojo, N. Su, Phys. Lett. B 720 (2013) 192;
K. Fukushima, Y. Hidaka, Phys. Rev. Lett. 110 (2013), 031601.
[45] J. Chao, P. Chu, M. Huang, Phys. Rev. D 88 (2013), 054009.
[46] D.U. Jungnickel, C. Wetterich, Phys. Rev. D 53 (1996) 5142.
[47] T.K. Herbst, J.M. Pawlowski, B.-J. Schaefer, Phys. Lett. B 696 (2011) 58.
[48] B.-J. Schaefer, J. Wambach, Nucl. Phys. A 757 (2005) 479.
[49] V. Skokov, B. Stokic, B. Friman, K. Redlich, Phys. Rev. C 82 (2010), 015206.
[50] V.I. Ritus, Ann. Phys. 69 (1972) 555;
C.N. Leung, S.Y. Wang, Nucl. Phys. B 747 (2006) 266.
[51] M. Frasca, Phys. Rev. C 84 (2011), 055208.
[52] G. Basar, D.E. Kharzeev, Phys. Rev. D 85 (2012), 086012.
[53] M. Ruggieri, Phys. Rev. D 84 (2011), 014011;
R. Gatto, M. Ruggieri, Phys. Rev. D 85 (2012), 054013.
[54] M.N. Chernodub, A.S. Nedelin, Phys. Rev. D 83 (2011), 105008.
[55] I.E. Frolov, V.C. Zhukovsky, K.G. Klimenko, Phys. Rev. D 82 (2010), 076002.
[56] R. Anglani, R. Casalbuoni, M. Ciminale, R. Gatto, N. Ippolito, M. Mannarelli, M. Ruggieri, arXiv:1302.4264 [hep-ph].
[57] E.S. Fraga, B.W. Mintz, J. Schaffner-Bielich, Phys. Lett. B 731 (2014) 154.